

Formation of an edge striped phase in the $\nu = \frac{1}{3}$ fractional quantum Hall system

E. V. Tsiper and V. J. Goldman

Department of Physics, State University of New York, Stony Brook, New York 11794-3800

(Received 26 December 2000; published 5 October 2001)

We have performed an exact diagonalization study of up to $N = 12$ interacting electrons on a disk at filling $\nu = \frac{1}{3}$ for both true Coulomb interaction, and the V_1 Haldane short-range interaction for which Laughlin wave function is the exact solution. For the Coulomb interaction and $N \geq 10$ we find persistent radial oscillations in electron density, which are not captured by the Laughlin wave function. Our results strongly suggest formation of a chiral striped phase at the edge of the fractional quantum Hall systems. The amplitude of the charge density oscillations decays slowly, only as a power law with the distance from the edge. Thus the spectrum of edge excitations is likely to be affected.

DOI: 10.1103/PhysRevB.64.165311

PACS number(s): 73.43.-f, 71.10.Pm

I. INTRODUCTION

An important open problem in the physics of the fractional quantum Hall effect (FQHE)^{1,2} is the structure and the properties of edge states. The bulk FQHE is reasonably well understood. The kinetic energy of two-dimensional (2D) electrons is quenched by the strong perpendicular magnetic field B , and the Coulomb interaction dominates the physics of the partially filled Landau level. At certain filling factors ν the electrons condense into highly correlated gapped quantum fluids, which results in quantization of the Hall conductance σ_{xy} and vanishing diagonal conductivity σ_{xx} .³ There has been much interest in the physics of FQH edge states for several reasons. First, on a QH plateau the bulk electron states are localized by disorder, and gapless excitations are possible only in extended edge states,^{4,5} thus the transport current flows along the edges.⁶ Second, FQH edge states have played an important role in many experiments: internal resonant tunneling from one edge to another through states bound on a quantum antidot has been employed to measure the fractionally quantized charge of the tunneling quasiparticles,⁷ and external electron tunneling into an edge of a FQH system has been used to study its excitation spectrum.⁸ Also, an edge channel is usually assumed to be localized within a few magnetic lengths $l_0 = \sqrt{\hbar c/eB}$ at the boundary of the FQH system, then the low-energy dynamics is effectively 1D, and field-theoretic descriptions of edge channels as a chiral Tomonaga-Luttinger liquid have been developed.^{9,10}

Our quantitative understanding of the FQHE is based on Laughlin wave function,² which is known to be quite accurate for the bulk, translationally invariant $\nu = \frac{1}{3}$ FQH state from extensive comparisons with exact diagonalization results in the edgeless spherical geometry.^{11,12} However, the accuracy of this wave function remains relatively untested at the edge. Validity of a wave function in the bulk does not necessarily extend to the edge: the ground state of the system is separated from excited states by a gap in the bulk, which makes it insensitive to perturbations; on the other hand, the system has gapless excitations at the edge, which makes it more susceptible to the particular form of the interelectron interaction. The FQHE has been relatively less studied in the disk geometry,^{2,13,14} because, in part, the interest was focused on the bulk states, and it is difficult to separate disk edge

effects for small number of electrons.

In this paper we report results of a detailed numerical investigation of the microscopic structure of the FQH edge. To this end, we diagonalize the interaction Hamiltonian in the disk geometry for up to $N = 12$ Coulomb-interacting electrons. For $N \geq 10$ we observe formation of a striped order in the charge density at the edges. These edge stripes are not captured by the Laughlin wave function that works well for the bulk FQH states. We also obtain an analytical fit to the numerical data, which suggests that the amplitude of the charge density oscillations decays only as a power law (specifically, as inverse square root) with distance, appreciably extending into the sample. We interpret these results as formation of an edge striped phase (ESP) with wave vector $q_{ESP} \approx \pi/2l_0$, possibly smectic liquid crystal, at the edge of a FQH system.

II. MODEL

We study the most simple FQH state at filling $\nu = \frac{1}{3}$, that of spin-polarized electrons restricted to lowest Landau level, as appropriate in the large B limit. In the symmetric gauge the vector potential is $\mathbf{A} = \frac{1}{2}[\mathbf{B}, \mathbf{r}]$, and the single-particle wave functions in the angular momentum representation are

$$\psi_m(\mathbf{r}) = (2\pi 2^m m!)^{-1/2} r^m e^{im\phi - r^2/4}, \quad (1)$$

where $m = 0, 1, 2, \dots$, and r (in units of l_0) and ϕ are the polar coordinates in the plane.

The interaction Hamiltonian in the second-quantized form is

$$\mathcal{H} = \sum_{mnl} V_{mn}^l c_{m+l}^\dagger c_n^\dagger c_{n+l} c_m, \quad (2)$$

where c_m^\dagger creates an electron in the single-particle eigenstate of the angular momentum ψ_m . There is no external confinement potential; the $\nu = \frac{1}{3}$ FQH state is chosen by setting the total angular momentum as described below. The Coulomb matrix elements V_{mn}^l are

$$\begin{aligned} V_{mn}^l &= \langle m+l, n | r_{12}^{-1} | m, n+l \rangle \\ &= \int \int d^2r_1 d^2r_2 \psi_{m+l}^*(\mathbf{r}_1) \psi_n^*(\mathbf{r}_2) \frac{1}{|\mathbf{r}_1 - \mathbf{r}_2|} \\ &\quad \times \psi_m(\mathbf{r}_1) \psi_{n+l}(\mathbf{r}_2). \end{aligned} \quad (3)$$

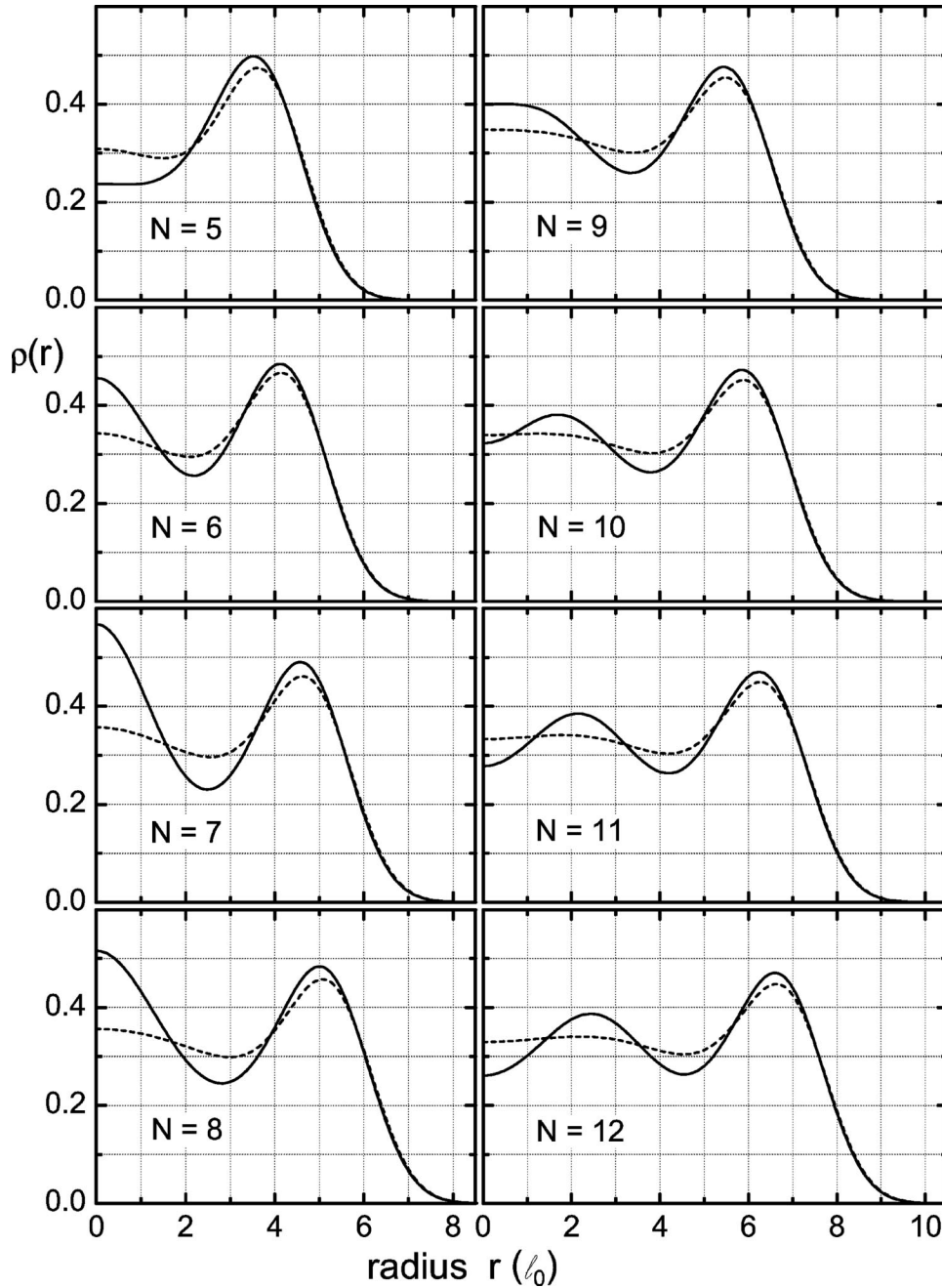


FIG. 1. Electron densities $\rho_L(r)$ and $\rho_C(r)$ for N interacting electrons in the disk geometry. The dashed lines show the Laughlin state for a short-range interaction, solid lines show the exact ground state for the Coulomb interaction.

We have found¹⁵ that the Coulomb matrix elements can be expressed via finite sums

$$V_{mn}^l = \sqrt{\frac{(m+l)!(n+l)! \Gamma(l+m+n+3/2)}{m!n! \pi 2^{l+m+n+2}}} \times [A_{mn}^l B_{nm}^l + B_{mn}^l A_{nm}^l], \quad (4)$$

where

$$A_{mn}^l = \sum_{i=0}^m \binom{m}{i} \frac{\Gamma(1/2+i)\Gamma(1/2+l+i)}{(l+i)! \Gamma(3/2+l+n+i)}, \text{ and} \quad (5a)$$

$$B_{mn}^l = \sum_{i=0}^m \binom{m}{i} \frac{\Gamma(1/2+i)\Gamma(1/2+l+i)}{(l+i)! \Gamma(3/2+l+n+i)} \left(\frac{1}{2} + l + 2i\right). \quad (5b)$$

The above equations are valid for $m, n, l \geq 0$. For matrix elements with negative $l < 0$ the identity $V_{mn}^{-l} = V_{m-l, n-l}^l$ can be used. These finite sums make the Coulomb-matrix elements significantly easier to compute than the expressions of Girvin and Jach.¹⁶

It is well known³ that the bulk ground state of N interacting electrons is well approximated by the Laughlin wave function

$$\Psi_L(z_1, \dots, z_N) = \prod_{j < k}^N (z_j - z_k)^3 \exp \left\{ - \sum_j^N \left| \frac{z_j}{2} \right|^2 \right\}, \quad (6)$$

where $z_j = x_j - iy_j$ (in units of l_0) gives the position of j th electron as a complex number. The Coulomb interaction Hamiltonian can be expressed as

$$V(|z_j - z_k|) = \sum_l V_l P_l^{jk}, \quad (7)$$

where V_l are the Haldane pseudopotentials, and P_l^{jk} is the projection operator that selects the states in which particles j and k have relative angular momentum l . The Laughlin wave function is known to be the exact ground state^{11,17,18} of the electrons interacting via a short-range potential when only V_1 is nonzero. The corresponding matrix elements for the short-range interaction Hamiltonian were obtained following Kasner and Apel.¹⁹

$$V_{mn}^{\text{SRI}} = \frac{\pi(m+n+l-1)! [(m-n)^2 - l^2]}{2^{m+n+l+2} \sqrt{m!n!(m+l)!(n+l)!}}. \quad (8)$$

III. RESULTS

We construct Ψ_L and Ψ_C numerically as the ground states of the short-range and Coulomb Hamiltonians, respectively, for the total angular momentum $M = \frac{3}{2}N(N-1)$ for N electrons, which gives filling $\nu = \frac{1}{3}$ in thermodynamic limit $N \rightarrow \infty$. The Hilbert space is restricted by consideration of single-particle orbitals with angular momentum $m \leq m_{\text{max}}$ only. For V_1 short-range interaction, the contribution of orbitals with $m > m_{\text{max}}^L = 3(N-1)$ vanishes identically; for Coulomb interaction m_{max}^C is obtained by increasing Hilbert space until overlap $\langle \Psi_L | \Psi_C \rangle$ converges to at least three significant digits. For example, for $N=12$, the largest $\nu = \frac{1}{3}$ FQH system studied, $M=198$ and the size of the Hilbert space is 15, 293, 119 for $m_{\text{max}}^C = 35$. To the best of our knowledge, the largest $\nu = \frac{1}{3}$ systems studied in the disk geometry prior to this study was $N=10$ by Cappelli *et al.*,¹⁴ who used only V_1 interaction.

In Fig. 1 we present the radial electron density profiles ρ_L and ρ_C for both Ψ_L (short-range interaction) and Ψ_C (true Coulomb interaction) for $N=5$ to 12 electrons. A comparison of $\rho_L(r)$ with the exact Coulomb $\rho_C(r)$ should clarify the importance of the long-range part of the Coulomb interaction for the FQH edge structure. For all N , the exponential fall off of $\rho_C(r)$ at the edge and the density oscillation nearest the edge is captured well by the Laughlin $\rho_L(r)$. As expected, the edge shifts to larger r in accordance with $r_{\text{edge}} \approx (2m_{\text{max}}^L)^{1/2}$. The properly normalized overlaps $\langle \Psi_L | \Psi_C \rangle$ are given in Table I. The corresponding overlaps are much closer to unity in the spherical geometry, which indicates that the deviation originates in the disk edge. Still, given the huge size of the Hilbert space, the overlaps indicate that Laughlin Ψ_L capture the important short-range FQH correlations remarkably well, even at the edge. Table I also gives W , the weight of the components of Ψ_C with $m > m_{\text{max}}^L$. All $W < 1\%$, which means that fixing total angular momentum

TABLE I. Normalized overlaps of the Laughlin ground state Ψ_L with the exact Coulomb ground state Ψ_C , and the Coulomb ground state in the restricted Hilbert space Ψ_{Cr} for N electrons. For Ψ_{Cr} the single-particle angular momentum m is restricted to $m \leq m_{\text{max}}^L$, where m_{max}^L is for Ψ_L . Here W is the weight of the components in the exact Ψ_C with $m > m_{\text{max}}^L$.

N	$\langle \Psi_L \Psi_{Cr} \rangle$	$\langle \Psi_L \Psi_C \rangle$	$10^3 \times W$
3	0.993606	0.990997	3.81
4	0.983108	0.978804	5.20
5	0.988168	0.985047	4.10
6	0.986102	0.981767	4.61
7	0.964758	0.956392	6.92
8	0.968652	0.962187	6.49
9	0.972992	0.966526	6.61
10	0.971415	0.964413	7.08
11	0.966118	0.958138	7.42
12	0.961240	0.9529 ^a	7.5 ^a

^aFor $N=12$ “unrestricted” overlap was obtained by an extrapolation, using the results for $m_{\text{max}}^C \leq m_{\text{max}}^L + 2$.

$M = \frac{3}{2}N(N-1)$ selects the $\nu = \frac{1}{3}$ state for Coulomb interaction too: it fixes average density on the disk $\langle \rho_C \rangle \approx \langle \rho_L \rangle$ (for $r < r_{\text{edge}}$) to better than 10^{-3} .

IV. ANALYSIS AND DISCUSSION

For $N=6$ to 8, density profile ρ_C clearly displays a commensurability effect, strongest for $N=7$, which can be visualized in a classical picture as tendency to have one central electron at $r=0$ surrounded by a ring of six electrons. For $N=7$ the position of the outer maximum in the density profile is very close to the lattice constant $a_{WC} = (4\pi\sqrt{3})^{1/2}l_0 \approx 4.665l_0$, of the $\nu = \frac{1}{3}$ 2D Wigner crystal in the thermodynamic limit.²⁰ This commensurability effect is barely visible for the Laughlin density profile $\rho_L(r)$, indicating importance of the long-range part of Coulomb interaction for formation of an ordered phase, even for such small electron systems.

For $N \geq 10$ the Laughlin state Ψ_L develops a constant density plateau $\rho_L \approx \frac{1}{3}$ in the interior of the disk. This is the precursor of the translationally and rotationally invariant $\nu = \frac{1}{3}$ bulk FQH condensate. Surprisingly, a second oscillation in the Coulomb $\rho_C(r)$ becomes evident for $N=10$; the second oscillation shifts to larger r as N is increased, following the first oscillation. The second oscillation is clearly caused by the long-range part of the Coulomb interaction, in other words, by the Haldane pseudopotentials V_l with $l \geq 3$ (because of Fermi statistics, l must be odd for spin-polarized electrons). In view of large overlaps, one may want to describe the edge charge density oscillations in Ψ_C in terms of excitations of Ψ_L by the long range part of the Coulomb interaction. Since the charge and the angular momentum M of the total system are fixed, a relevant elementary excitation to consider is a quasiparticle-quasihole bound exciton.²¹ The excitations that do not conserve m are not relevant because they alter M . A variational wave function that admixes one bound exciton into Ψ_L reproduces charge density oscillations

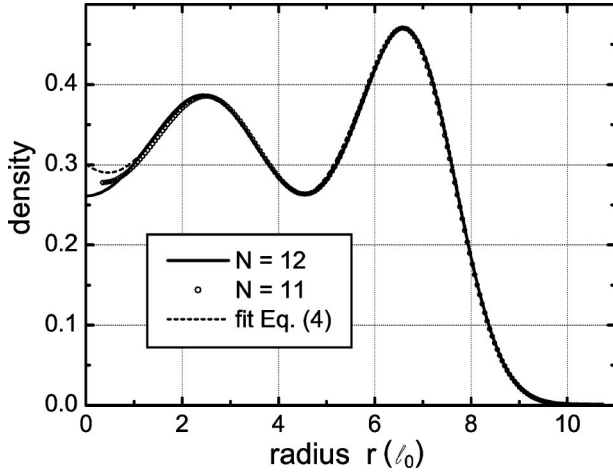


FIG. 2. Electron density $\rho_C(r)$ for N Coulomb-interacting electrons. The $N=11$ density data (circles) is shifted radially by $r_{\text{edge}}(N=12) - r_{\text{edge}}(N=11) \approx 0.378$. The dashed line is the fit of Eq. (10) with parameters given in the text.

in $\rho_C(r)$ for $N=10$ to 12 reasonably well.²² The deviation of the variational $\rho(r)$ from the exact $\rho_C(r)$ increases, however, as N is increased from 10 to 11 to 12 , which indicates that more than one bound exciton is needed for larger systems.

We have obtained a good phenomenological fit of the exact $\rho_C(r)$ dependence using an analytical expression:

$$\rho(r) = \rho_0 [(\text{erf } \bar{r} + 1)/2] \{1 + \rho_{ESP0} J_0[q_{ESP}(\bar{r} - \bar{r}_0)]\}, \quad (9)$$

where $\rho_0 = \frac{1}{3}$ for $\nu = \frac{1}{3}$, $\bar{r} = r_{\text{edge}} - r$ is the distance from the edge in units of l_0 , $\text{erf}(x)$ is the Gauss error function, and J_0 is the Bessel function of the first kind. The fitting parameters are the ESP oscillation amplitude at the edge ρ_{ESP0} , the ordering wave vector q_{ESP} , and the shift of the first oscillation from the edge \bar{r}_0 . The fit is robust in the sense that the same fitting parameters also give good fits for $N=10$ and 11 , scaling r_{edge} as $(2m_{\text{max}}^L)^{1/2}$. A fit for $N=11, 12$ is shown in Fig. 2, where the values of the parameters are $\rho_{ESP0} = 0.519$, wave vector $q_{ESP} = 1.570/l_0$, and $\bar{r}_0 = 0.99$. We believe that the deviation of the fit from the exact density in the center of the disk for $r < 1$ is a finite-size effect. The parameters ρ_{ESP0} and \bar{r} may be varied by 1% to give equally good overall fit. The wavelength $\lambda_{ESP} = 4.002$ can be compared to several natural lengths in the problem. It is significantly smaller than the Wigner crystal-lattice constant $a_{WC} = (4\pi\sqrt{3})^{1/2} \approx 4.665$, and, more relevant, is accurately equal to the distance between the crystal planes $h_{WC} = (\sqrt{3}/2)a_{WC} = (3\pi\sqrt{3})^{1/2} \approx 4.040$. We also note that q_{ESP} is close to the wave vector of the bulk magnetoroton minimum q_{MR} .²³ Similar length scales are provided by many other quantities, e.g., the ‘‘ion diameter’’ $2R_0 = \sqrt{6\pi} \approx 4.342$, a little too large; square root of the ‘‘disk area per electron’’ $(2\pi m_{\text{max}}^L/N)^{1/2} = [6\pi(N-1)/N]^{1/2} \approx 4.157$ for $N=12$ is closer, but the $\rho_C(r)$ data do not show such dependence on N , Fig. 2.

In the disk geometry rotational symmetry (corresponding to translational invariance *along* a linear edge) of the chiral basis orbitals ψ_m ensures that azimuthal density modulations in $\rho(\theta)$ are not possible. A broken symmetry ground state is possible only as a superposition of several rotationally invariant *degenerate* ground states at different total M . Such ground state would be pinned by disorder and QHE would not be observable in experiments. A charge density wave (CDW) order is possible in the radial direction, however; in the thermodynamic limit,²⁴ the edge confinement breaks the translational invariance and ‘‘excites’’ radial CDW. Because of the long-range nature of the Coulomb interaction, the radial CDW is expected to propagate deep into the interior of the electron system and form a locally anisotropic edge striped phase (ESP). Since there is abundant experimental evidence that FQH edges are conducting, ESP is a conductor along the edge, and an insulator in the perpendicular direction, in the sense that in a QH system radial perturbation will induce only azimuthal Hall current. Thus, ESP can be thought of as a quantum smectic liquid crystal phase²⁵ at the edge of the system.

Extrapolating to the thermodynamic limit, and setting $\rho_{ESP0} = \frac{1}{2}$, $q_{ESP} = \pi/2$, the following simple expression describes well the electron density at the $\nu = \frac{1}{3}$ FQH edge:

$$\rho(y) = \frac{1}{6} (\text{erf } y + 1) \left\{ 1 + \frac{1}{2} J_0 \left[\frac{\pi}{2} (y - 1) \right] \right\}, \quad (10)$$

where y is the distance from the edge. In the disk geometry the azimuthal transport current density $J_\phi \propto \partial_r \rho(r)$. Differentiating Eq. (10) we obtain edge current density

$$J_x(y) \propto \frac{1}{3\sqrt{\pi}} (e^{-y^2}) \left\{ 1 + \frac{1}{2} J_0 \left[\frac{\pi}{2} (y - 1) \right] \right\} - \frac{\pi}{24} (\text{erf } y + 1) J_1 \left[\frac{\pi}{2} (y - 1) \right]. \quad (11)$$

In practice, the first term with $\exp(-y^2)$ vanishes after the first oscillation. The phenomenological expressions Eqs. (10) and (11) are plotted in Fig. 3. Large y asymptotic behavior of both Bessel functions is $\propto y^{-1/2} \cos(\pi y/2)$ (with a $\pi/2$ phase shift). Thus, should Eqs. (10) and (11) prove applicable to linear edges in large systems, the amplitudes of the charge density and the transport current oscillations both decay only as a power law of distance from the edge, specifically as $y^{-1/2}$. We note that the $\propto y^{-1/2}$ asymptotic behavior is not well established for the thermodynamic limit; the exponent of the power law may be affected by the geometry effects of a small disc in our numerical results.

V. IMPLICATIONS

There are likely to be several important implications of the observed slow-decaying charge density oscillations at FQH edges. Note first that they do not affect topological QHE properties, such as the values of the quantized σ_{xy} , Ref. 1, and the charge of the bulk Laughlin quasiparticles.⁷ On the other hand, dynamic properties, where edge excitations at finite frequency and wave vector are important, are

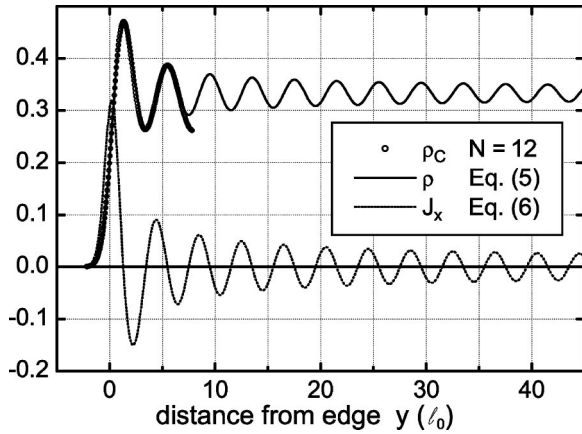


FIG. 3. Electron density and transport current density (arb. units) vs distance from the $\nu = \frac{1}{3}$ FQH edge. Density $\rho_C(r)$ for 12 electrons is also shown. The analytical expressions Eqs. (10) and (11) are inferred from the numerical data.

likely to be affected. For example, since edge excitations are expected to be transverse charge density waves,⁹ it seems that the presence of ESP at QH edges should affect spectrum of edge excitations.^{8,27} The striped phase may be the reason for the reported experimental dependence of velocity of

propagation of edge magnetoplasmons on frequency.²⁶ When there are several edge modes present, a striped phase extending hundreds of l_0 from the edge is likely to couple various modes, and this may explain the failure to observe multiple and/or counterpropagating modes in experiments.²⁶

A complementary field-theoretic approach for the dynamics of an edge channel treats it as a Luttinger liquid, focusing on the asymptotic long-distance, low-energy physics.^{9,10} It has been argued that many expected power law behaviors in this limit are completely determined by the quantized value of σ_{xy} , and would not be affected by the specifics of the edge structure. The mapping of a FQH edge onto the Luttinger liquid is based on rather general considerations, *provided* there is no $\propto 1/r$ interparticle interaction. In this work we specifically show that the long-ranged true Coulomb interaction leads to formation of a striped phase at the $\nu = \frac{1}{3}$ FQH edge, calling into question the fundamental assumption that all important physics at the edge is one dimensional.

ACKNOWLEDGMENTS

We are grateful to I. L. Aleiner and J. K. Jain for discussions. This work was supported in part by the NSF under Grant No. DMR9986688.

- ¹D.C. Tsui, H.L. Stormer, and A.C. Gossard, Phys. Rev. Lett. **48**, 1559 (1982).
- ²R.B. Laughlin, Phys. Rev. Lett. **50**, 1395 (1983).
- ³Reviewed in: *The Quantum Hall Effect*, 2nd ed., edited by R.E. Prange and S.M. Girvin (Springer, New York, 1990); *Perspectives in Quantum Hall Effects*, edited by S. Das Sarma and A. Pinczuk (Wiley, New York, 1997); S.M. Girvin, in *The Quantum Hall Effect, 1998*, Les Houches Lecture Notes (EDP Sciences, Paris, 1999).
- ⁴R.B. Laughlin, Phys. Rev. B **23**, 5632 (1981).
- ⁵B.I. Halperin, Phys. Rev. B **25**, 2185 (1982).
- ⁶J.K. Wang and V.J. Goldman, Phys. Rev. Lett. **67**, 749 (1991); Phys. Rev. B **45**, 13 479 (1992).
- ⁷V.J. Goldman and B. Su, Science **267**, 1010 (1995); Physica E (Amsterdam) **1**, 15 (1997).
- ⁸M. Grayson, D.C. Tsui, L.N. Pfeiffer, K.W. West, and A.M. Chang, Phys. Rev. Lett. **80**, 1062 (1998).
- ⁹X.G. Wen, Intl. J. Mod. Phys. B **6**, 1711 (1992).
- ¹⁰M. Stone, Phys. Rev. B **42**, 8399 (1990).
- ¹¹F.D.M. Haldane, Phys. Rev. Lett. **51**, 605 (1983).
- ¹²S. He, X.C. Xie, and F.C. Zhang, Phys. Rev. Lett. **68**, 3460 (1992).
- ¹³G. Dev and J.K. Jain, Phys. Rev. B **45**, 1223 (1992).
- ¹⁴A. Cappelli, C. Mendez, J. Simonin, and G.R. Zemba, Phys. Rev.

- B **58**, 16 291 (1998).
- ¹⁵E. V. Tsiper (unpublished).
- ¹⁶S.M. Girvin and T. Jach, Phys. Rev. B **29**, 5617 (1984).
- ¹⁷S.A. Trugman and S. Kivelson, Phys. Rev. B **31**, 5280 (1985).
- ¹⁸F.D.M. Haldane, in *The Quantum Hall Effect*, Ref. 3.
- ¹⁹M. Kasner and W. Apel, Ann. Phys. (Leipzig) **3**, 433 (1994).
- ²⁰It is well known that the ground state at $\nu = \frac{1}{3}$ cannot be a Wigner crystal without Landau level mixing, in the high B limit.
- ²¹R.B. Laughlin, Physica B & C **126**, 254 (1984).
- ²²S. S. Mandal and J. K. Jain (private communication).
- ²³S.M. Girvin, A.H. MacDonald, and P.M. Platzman, Phys. Rev. B **33**, 2481 (1986).
- ²⁴In the thermodynamic limit the azimuthal angle ϕ degree of freedom maps onto coordinate x along the linear edge, and the radius r maps onto y transverse to the edge. We also note that confinement by fixing M is very sharp; electron confinement by a shallow external potential V_{ext} (small gradient: $l_0 \partial_r V_{\text{ext}} \ll \Delta_{\text{gap}}$) may reduce amplitude of the edge striped phase, but can also lead to a phase separation.
- ²⁵S.A. Kivelson, E. Fradkin, and V.J. Emery, Nature (London) **393**, 550 (1998).
- ²⁶N.B. Zhitenev *et al.*, Phys. Rev. B **49**, 7809 (1994), and references therein.
- ²⁷V.J. Goldman and E.V. Tsiper, Phys. Rev. Lett. **86**, 5841 (2001).